Doxorubicin-loaded PLGA nanoparticles for the chemotherapy of glioblastoma: Towards the pharmaceutical development

Olga Maksimenko[a], Julia Malinovskaya[a,b], Elena Shipulo[a], Nadezhda Osipova[a], Victoria Razzhivina[a], Diana Arantseva[a], Oksana Yarovaya[c], Ulyana Mostovaya[c], Alexander Khalansky[d], Vera Fedoseeva[d], Anna Alekseeva[d,e], Ludmila Vanchugova[f], Marina Gorshkova[f], Elena Kovalenko[g], Vadim Balabanyan[a,b], Pavel Melnikov[h], Vladimir Baklaushev[i], Vladimir Chekhonin[h], Jörg Kreuter[e,j], Svetlana Gelperina[a,*]

[a] Drugs Technology LLC, Rabochaya ul. 2A, 141400 Khimki, Moscow Region, Russia
[b] Lomonosov Moscow State University, ul. Leninskiye Gory, 119991 Moscow, Russia
[c] D. Mendeleev University of Chemical Technology of Russia, Miusskaya pl. 9, 125047 Moscow, Russia
[d] Institute of Human Morphology, Russian Academy of Sciences, ul. Tsurupy 3, 117418 Moscow, Russia
[e] I.M. Sechenov First Moscow State Medical University, B. Pirogovskaya ul., 19-1, 119146 Moscow, Russia
[f] Topchiev Institute of Petrochemical Synthesis, Russian Academy of Sciences, Leninsky pr. 29, 19991 Moscow, Russia
[g] Shemyakin-Ovchinnikov Institute of Bioorganic Chemistry, Russian Academy of Sciences, ul. Miklukho-Maklaya, 16/10, bldg 7, 117198 Moscow, Russia
[h] V. Serbsky Federal Medical Research Centre of Psychiatry and Narcology of the Ministry of Health of the Russian Federation, Kropotkinskiy per. 23, 119034 Moscow, Russia
[i] Federal Research and Clinical Center of Specialized Medical Care and Medical Technologies, Federal Biomedical Agency of the Russian Federation, Orekhoviy blvd. 28, 115682 Moscow, Russia
[j] Institute of Pharmaceutical Technology, Biocenter, Goethe University, Max-von-Laue-Str. 9, 60438 Frankfurt/Main, Germany

ARTICLE INFO

ABSTRACT

Brain delivery of drugs by nanoparticles is a promising strategy that could open up new possibilities for the chemotherapy of brain tumors. As demonstrated in previous studies, the loading of doxorubicin in poly(lactide-co-glycolide) nanoparticles coated with poloxamer 188 (Dox-PLGA) enabled the brain delivery of this cytostatic that normally cannot penetrate across the blood-brain barrier in free form. The Dox-PLGA nanoparticles produced a very considerable anti-tumor effect against the intracranial 101.8 glioblastoma in rats, thus representing a promising candidate for the chemotherapy of brain tumors that warrants clinical evaluation. The objective of the present study, therefore, was the optimization of the Dox-PLGA formulation and the development of a pilot scale manufacturing process. Optimization of the preparation procedure involved the alteration of the technological parameters such as replacement of the particle stabilizer PVA 30–70 kDa with a presumably safer low molecular mass PVA 9–10 kDa as well as the modification of the external emulsion medium and the homogenization conditions. The optimized procedure enabled an increase of the encapsulation efficiency from 66% to > 90% and reduction of the nanoparticle size from 250 nm to 110 nm thus enabling the sterilization by membrane filtration. The pilot scale process was characterized by an excellent reproducibility with very low inter-batch variations. The in vitro hematotoxicity of the nanoparticles was negligible at therapeutically relevant concentrations. The anti-tumor efficacy of the optimized formulation and the ability of the nanoparticles to penetrate into the intracranial tumor and normal brain tissue were confirmed by in vivo experiments.

1. Introduction

Glioblastoma multiforme (GBM), the most aggressive of the primary brain tumors, is relatively rare with the incidence of ~3 per 100,000 people (Ostrom et al., 2018); however, it is also the most common CNS malignancy with dismal prognosis. The standard treatment protocol of newly diagnosed GBM involves maximal possible resection followed by radiotherapy and adjuvant chemotherapy. Despite this aggressive treatment, the incidence of recurrence is very high leading to median overall survival of only 15–23 months and 5-year survival of less than

6% (Ostrom et al., 2018; Shergalis et al., 2018).

Beyond many genetic and epigenetic modifications leading to chemo- and radioresistance, recurrence of GBM occurs due to its infiltrative growth pattern that impedes the complete surgical resection leading to further invasion of surviving tumor cells. Only a limited number of patients with recurrent tumors are eligible for a second resection and its benefit is not clear (van Linde et al., 2017), whereby the effectiveness of chemotherapy is limited largely due to insufficient brain delivery of most therapeutics across the blood-brain barrier (BBB) (van Tellingen et al., 2015). As evidenced by the T1 contrast-enhanced magnetic resonance images, the integrity of the BBB is compromised within the tumor core so that the systemically administered solutes – gadolinium-based contrast agents and drugs – that normally do not freely penetrate across the BBB get access to the tumor. At the same time, as shown by numerous imaging and biopsy studies, gliomas diffuse beyond the contrast-enhanced areas to the areas where the function of the BBB is still retained (Gerstner et al., 2010; Eidel et al., 2017). Notably, it is in these peritumoral areas where the majority of tumor recurrences occur (Lemée et al., 2015; Vehlow and Cordes, 2013; Petrecca et al., 2013). Overall, these observations suggest that the BBB is a paramount obstacle preventing the access of potentially effective drugs to the peritumoral zone. Therefore, a technology enabling the delivery of drugs to those brain regions that are still protected by the functional BBB but prone to invasion of tumor cells will help to gain long-term tumor control.

Brain delivery of drugs by nanoparticles is a promising strategy that could offer a solution for this problem. Our previous studies demonstrated that the intravenously injected poly(lactide-co-glycolide) (PLGA) nanoparticles coated with poloxamer 188 enabled the brain delivery of model drugs – loperamide and doxorubicin that cannot penetrate across the BBB in the free form (Gelperina et al., 2010; Wohlfart et al., 2011). It is hypothesized that in the blood the poloxamer 188 coating enhances the adsorption of certain apolipoproteins (most likely E, B, and A-1) to the nanoparticle surface, and then these carriers – now mimicking lipoprotein particles – find their way into the brain via receptor-mediated endocytosis following the routes of lipoproteins that deliver to the brain exogenous lipids (reviewed in: Kreuter, 2014).

Doxorubicin is one of the most effective antitumor drugs that is used – alone or in combinations – as the first-line therapy in many cancers. It is also a drug of choice in a great number of drug delivery-related studies that are aimed at overcoming tumor resistance to this drug and diminishing its adverse effects by a more selective tumor delivery (reviewed in: Kanwal et al., 2018; Cagel et al., 2017). In our studies aimed at the development of brain delivery systems, doxorubicin was chosen as a model drug on one hand because of its potential anti-tumor effect against gliomas (Voulgaris et al., 2002; Tomita, 1991) and on the other hand because of its inability to penetrate across the BBB in therapeutically effective concentrations (von Holst et al., 1990). The loading of doxorubicin in the PLGA nanoparticles coated with poloxamer 188 enabled a very considerable anti-tumor effect against the intracranial 101.8 glioblastoma in rats manifested as a significant inhibition of tumor growth and increase in survival time (Gelperina et al., 2010; Wohlfart et al., 2011). This high efficacy suggested that the nanoparticle-based formulation of doxorubicin is a promising candidate for the chemotherapy of brain tumors that warrants clinical evaluation.

In the present paper we, therefore, describe the results of the studies aimed at the optimization of the doxorubicin formulation based on the PLGA nanoparticles and of the pilot scale manufacturing process that could facilitate its industrial manufacturing and further clinical investigations.

2. Materials and methods

2.1. Preparation of nanoparticles

2.1.1. Doxorubicin-loaded PLGA nanoparticles (Dox-PLGA)
The nanoparticles were prepared by a double emulsion solvent evaporation technique (w/o/w). Briefly, poly(lactide-co-glycolide) with acid end groups (500 mg, Resomer® 502H, D,L-lactide/glycolide = 50:50 mol/mol; Mw 7–17 kDa, η = 0.21 dL/g, Evonik Röhm GmbH, Germany) was dissolved in 3 ml of dichloromethane (DCM). Doxorubicin hydrochloride (Teva, Sicor, Italy) was dissolved in 0.001 N HCl to a final concentration of 23 mg/ml or 12.5 mg/ml. The solutions were mixed and emulsified using a high shear homogenizer (Ultra-Turrax T18 Basic, IKA, Germany) to obtain primary emulsion (w/o) with a drug-to-polymer ratio of 1:10 or 1:20 (w/w). The primary emulsion was added into a 1% solution of polyvinyl alcohol (PVA, 9–10 kDa, 80% hydrolysed, Sigma, Steinheim, Germany) in phosphate-buffered saline (PBS, pH7.4), if not mentioned otherwise, and emulsified using a high shear homogenizer (Ultra-Turrax T18) followed by high-pressure homogenization at 1000 bar (5 min, PandaPLUS 2000, Gea Niro Soavi, Italy; 3 min, Microfluidizer M-110P, Microfluidics, Newton, MA, USA). The phase volume ratio of the double emulsion was w/o/w = 2:3:25. The organic solvent was removed under vacuum (to 25 mbar) using a rotary evaporator; the resulting suspension was filtered through a glass porous filter and freeze-dried with 5% of mannitol as a cryoprotectant. The freeze-dried nanoparticles were stored at 4 °C.

Additionally, the Dox-PLGA nanoparticles were prepared using alternative PVA grades: PVA 30–70 kDa, 88% hydrolyzed (Sigma-Aldrich, Germany); PVA 15 kDa, fully hydrolyzed (Merck Millipore, Germany); PVA 13 kDa, 96% hydrolysed (Sigma-Aldrich, Germany). Other experimental parameters remained the same.

2.2. Characterization of nanoparticles

Evaluation of drug content and encapsulation efficiency. To determine the drug content, the freeze-dried nanoparticles were dissolved in DMSO. The doxorubicin concentration was measured spectrophotometrically at 481 nm using a calibration curve in the concentration range from 0.00 to 20.0 µg/ml (correlation coefficient $R^2 = 0.998837$).

The concentration of free doxorubicin was measured spectrophotometrically after separation of the nanoparticles by centrifugation. The nanoparticles were resuspended in distilled water, and then the suspension was centrifuged at 48,380 g for 30 min at 5 °C (Avanti JXN-30, USA). The doxorubicin concentration in the filtrates was measured spectrophotometrically at 481 nm using a calibration curve in the concentration range from 0.00 to 20.0 µg/ml (A = 0.01808 × C, correlation coefficient R2 = 0.99809).

Drug encapsulation efficiency (EE, %) was calculated as:

$$EE(\%) = [(C_{total} - C_{free}): C_{total}] \times 100\%,$$

where: EE (%) – encapsulation efficiency, C_{total} (mg/ml) – total doxorubicin concentration in the sample, C_{free} (mg/ml) – concentration of free doxorubicin.

The doxorubicin yield (Y, %) was calculated as the ratio between the theoretical and the determined doxorubicin concentrations in the suspension.

All measurements were performed in triplicates.

Measurement of nanoparticle size and size distribution and zeta-potential. The average size and the polydispersity index (PDI) of the nanoparticles were measured by dynamic light scattering (DLS) using a Zetasizer NanoZS (Malvern Instruments, Malvern, UK). For size measurement, the freeze-dried nanoparticles were resuspended in purified deionized (Milli-Q) water. The zeta-potential was determined by microelectrophoresis in a dip cell. All measurements were performed in quadruplicates with 50-fold dilution of the suspension.

Study of drug release kinetics. The 24-h kinetics of doxorubicin release from the nanoparticles was studied using 0.9% NaCl solution as a release medium. In the continuous experiment (120 h incubation), a 1% poloxamer 188 (P188, Kolliphor® P188, BASF, Germany) solution was used as the release medium.

The freeze-dried nanoparticle samples were resuspended in either solution, then diluted 25-fold and incubated at 37 °C under continuous stirring at 200 rpm. At predetermined time points (0.5, 1, 2, 3, 4, 6, and 24 h) 1-ml aliquots were withdrawn, and the nanoparticles were separated by centrifugation (48,380 g for 30 min at 5 °C). The amount of released doxorubicin in supernatants was quantified spectrophotometrically (λ_{max} = 481 nm). Doxorubicin stability was controlled based on the spectra obtained at different time points. Each measurement was performed for three samples in parallel.

2.3. Interfacial tension measurement

The interfacial tension was measured in the model system consisting of a PLGA solution in dichloromethane and a doxorubicin solution in 1% PVA at 25 °C by the pendant drop technique using an EasyDrop contact angle measuring instrument DSA20E (KRÜSS GmbH, Germany). The heavier organic phase (16.7% PLGA solution in dichloromethane) was loaded into a syringe and introduced through a dosing needle into the experimental cell containing the lighter aqueous phase (0.2% or 1% solution of doxorubicin in 1% aqueous PVA solution). The interfacial tension was then determined from the shape of the pendant drop suspended at the tip of a needle. The drop images were digitalized with the aid of the video frame grabber of the camera and analyzed using Drop Shape Analysis (DSA1) software that infers the surface tension from the geometrical profile of the drop.

2.4. Irradiation of nanoparticles

Gamma irradiation of the nanoparticle samples was performed using a ^{60}Co source GU-150 (Joint Stock Company "Technical Physics and Automation Research Institute", Russia) with a gamma radiation energy of 1.25 MeV. The exposure rate was 2.0 Gy/s. Electron beam irradiation was performed using a linear electron accelerator U-003 (Scientific Production Association "NPO Toriy", Russia) with electron energy of 4.0 MeV (electron beam current up to 4 mA). The absorbed dose rate in the irradiated material was $1.6 \cdot 10^3$ Gy/s. The lyophilized samples of the doxorubicin-loaded PLGA NP (Dox-to-PLGA ratio = 1:10 or 10:20, w/w) and empty NP (PLGA-Placebo) were irradiated to the doses of 10, 15, and 25 kGy at ambient temperature. The influence of ionizing radiation on the physicochemical properties of nanoparticles as well as the stability of main formulation ingredients was investigated as described below using non-irradiated samples as controls.

The molecular mass distribution of PLGA before and after gamma irradiation was determined by gel permeation chromatography using a Waters HPLC system equipped with a UV detector (Milton Roy 3100) and a differential refractometer (Waters 2414) and a set of Styrogel HR5E and HR4E columns (300 × 7.8 mm). For analysis the polymer was dissolved in tetrahydrofuran (THF). The solvent was added into the vials with the irradiated samples, then after 2 h the mixture was filtered through the membrane filter (Chromafil Xtra PTFE 45/25, Macherey-Nagel GmbH & CoKG, Germany). The filtrates were diluted with THF to a concentration of ~1 mg/ml of PLGA. THF was used as an eluent at a flow rate of 1.00 ml/min; the system was equilibrated at 25 °C; injection volume was 50 µl. Data analysis was performed using the Z-lab software. The system was calibrated using a polystyrene standard set (Mp 500–955,000 Da, Waters, USA).

Doxorubicin stability (content of the substance and impurities) in the irradiated nanoparticles was evaluated by HPLC. The irradiated and non-irradiated nanoparticle samples (1 ml lyophilizate per vial) were resuspended in distilled water (150 µl); then acetonitrile (700 µl) was added, and the obtained mixture was placed for 3 min in the ultrasonic bath. Insoluble precipitates were separated by centrifugation (9000 rpm, 3 min), and the supernatants were analyzed by HPLC (Agilent 1200 LC system, column Zorbax SB-C18, 150 × 3 mm, 3.5 µm). A mixture of a buffer solution (2.88 g of SDS and 2.25 g of phosphoric acid per 1 L of solution) and acetonitrile at a ratio of 56:44 (v/v) was used as a mobile phase at a flow rate of 0.9 ml/min. The column temperature was 40 °C. Data were collected using a spectrophotometric detector at 254 nm.

2.5. Manufacturing of the pilot batch

Doxorubicin hydrochloride (4.22 g, Teva Sicor, Italy) was dissolved in 165 ml of 0.001 N HCl. The resulting solution was added to a solution of PLGA (40 g, Resomer® 502H) in dichloromethane (252 ml), and then the mixture was homogenized using an Ultra Turrax T-25 (23,000–24,000 rpm, 5 min). The obtained pre-emulsion (w/o) was then added to 2 L of a 1% PVA (9–10 kDa, 80% hydrolysed, Sigma, Steinheim, Germany) solution in 0.01 M phosphate buffer (PB: 8 mM Na_2HPO_4, 2 mM KH_2PO_4, pH 7.4) under stirring, homogenized using an Ultra Turrax T-25 (23,000–24,000 rpm, 20 min), and then passed through a high-pressure homogenizer (M-110 Microfluidizer®, Microfluidics Corp., MA, USA) at 1000 bar. The homogenization cycle was repeated three times (3 × 30 min). Then dichloromethane was evaporated under reduced pressure (90 min), and mannitol (5%) was added to the resulting aqueous suspension. The final suspension was subjected to continuous flow centrifugation (30,000 rpm, processing time 102 s, CEPA GLE High-Speed Tubular Centrifuge, John Morris Scientific Pty Ltd., Eppendorf) to separate bigger particles or agglomerates.

The supernatant was filtered through a sterile filter unit (PES Capsule sterile filters 0.2 µm, M3, Lenntech, Germany). The sterilized nanosuspension containing ~1.5 mg/ml of doxorubicin was filled in 25-ml glass vials (25 mg of doxorubicin and 850 mg of mannitol in a vial), freeze-dried, and stored at 4 °C. Sterility of the lyophilized samples was tested using the method of membrane filtration according to the pharmacopoeia requirements.

2.6. Evaluation of hemocompatibility

The hemocompatibility of the doxorubicin-loaded nanoparticles was evaluated using human venous blood from three healthy volunteer donors. Written informed consent was obtained from all volunteers, and the study was approved by the Ethics Committee of the Federal Research and Clinical Center of Specialized Medical Care and Medical Technologies, Federal Biomedical Agency of the Russian Federation. Whole blood was collected into tubes containing sodium citrate as anticoagulant. The Dox-PLGA-p.s. formulation (pilot batch) with the following parameters was used for this study: average size 110 ± 1 nm; PDI 0.117 ± 0.003; zeta-potential −1.29 ± 0.35 mV; encapsulation efficiency 80%) and placebo PLGA NP (average size 116 ± 0 nm; PDI 0.192 ± 0.011; zeta-potential −12.4 ± 0.5 mV).

Blood coagulation study. Influence of the nanoparticles on the blood coagulation cascade was evaluated by measuring of the prothrombin time (PT) after plasma incubation with the PLGA-Dox and PLGA-Placebo nanoparticles at the concentrations of 1, 10, 100 µg/ml. The plasma fraction was isolated by centrifugation (1200–1500 g, 10 min, 25 °C). The blood samples were incubated with the nanoparticles for 30 min at 37 °C under continuous shaking and then placed into the coagulometer followed by the addition of calcium thromboplastin to activate the clot formation; afterwards measurement of the coagulation time was performed. Each sample was tested in triplicate.

Platelet-activation assay. To assess the NP thrombogenicity the level of platelet activation as a percentage of P-selectin expression on platelet surface was evaluated by flow cytometry. Platelet-rich plasma (PRP) was obtained by centrifugation (1000 rpm; 10 min) of freshly derived human whole blood. Then the PRP was incubated with the

nanoparticles in the concentration range of 0.1–100 µg/ml. PRP incubated with the platelet aggregation inductor (platelet aggregation inductor adenosine diphosphate, ADP) was used as a positive control. Platelet samples were then incubated with FITC-conjugated anti-CD36 and PE-conjugated anti-CD62 (anti-P-selectin) antibodies (10 µg/ml, Biolegend, USA) to determine platelet cell population and activated platelets, respectively. Afterwards the samples were diluted with the fluorescence-activated cell sorting fluid and analyzed by flow cytometry.

Assay of hemolysis. The blood samples were incubated with the PLGA-Dox and PLGA-Placebo nanoparticles in the concentrations of 1, 10, and 100 µg/ml for 3 h at 37 °C. Then the samples were centrifuged (800 g, 15 min) to separate non-damaged erythrocytes, and the concentration of free hemoglobin in the supernatant was determined spectrophotometrically at 540 nm. The total hemoglobin concentration in the blood samples was determined after addition of Triton X-100 (positive control). The results are expressed as the percentage of hemolysis.

2.7. In vivo studies

The in vivo experiments were performed in accordance with the European Convention for the Protection of Vertebrate Animals, Directives 86/609/EEC, recommendations of the FELASE working group (1986, 86/609/EEC, ISSN 03780 6978), and the National standard of the Russian Federation R 53434-2009 "Good Laboratory Practice".

All experiments were performed using adult male Wistar rats weighing 200–220 g obtained from the animal production unit of the Russian Academy of Sciences (Stolbovaya, Moscow Region, Russia). The rats were caged in groups of six and maintained on a standard 12-h light-dark cycle. They received standard laboratory food and water *ad libitum* throughout the study.

2.7.1. Evaluation of anti-tumor effect in an orthotopic 101/8 glioblastoma model

Tumor model. The intracranial implantation of the rat 101/8 glioblastoma was performed using fresh tumor tissue as described by Steiniger et al. (2004). The animals were anaesthetized by intraperitoneal injections of 100 mg/kg ketamine and 10 mg/kg xylazine. To induce the tumor, a piece of tumor tissue (~10^6 tumor cells) from the frozen stock (collection of the Institute of Human Morphology, Moscow, Russia) was introduced into a cavity of the right lateral ventricle of donor animals using a tuberculin syringe (B. Braun, Melsungen, Germany). Through a midline sagittal incision, a burr hole of 1.5 mm in diameter was made with a dental drill 2 mm lateral to the sagittal midline and 2 mm posterior to the right coronal suture. Surgical glue (Turbo 2000 Kleber Universal, Boldt Co, Wermelskirchen, Germany) was used to close the scalp incision. The animals were euthanized by carbon dioxide asphyxiation after development of the pronounced clinical signs of illness (usually day 14 to day 18), and the brains were removed. The tumor tissue was excised and homogenized with a scalpel. The aliquots of fresh tumor tissue were implanted into the brains of new experimental animals as described above.

Chemotherapy of 101/8 rat glioblastoma. Tumor-bearing animals were randomly divided into groups (n = 10) to receive the Dox-PLGA nanoparticles coated with poloxamer 188 produced on the pilot scale (Dox-PLGA-p.s.) or a solution of doxorubicin hydrochloride in water (Dox). The formulations were administered by intravenous injection into the tail vein in the dose of 3 × 1.5 mg/kg (as doxorubicin) on days 2, 5, and 8 after tumor implantation. Coating of the nanoparticles with poloxamer 188 (P188) was performed immediately before the injection. For coating, the nanoparticulate formulations were resuspended in 1% aqueous solution of P188 followed by incubation for 30 min at 20 °C. Untreated animals were used as controls. The animals were sacrificed on day 14 post implantation. The brains were carefully removed and

processed for histological analysis.

Measurement of tumor size. Preparation of the histological slides was performed as described by Wohlfart et al. (2009). For the histological evaluation, the brains were fixed in 3.75% zinc formalin solution (Thermo Shandon, Pittsburgh, USA) for at least 48 h at room temperature and afterwards embedded in paraffin. A routine haematoxylin and eosin staining on 5 mm thick sections was performed. Sections were scanned using a high resolution scanner Epson Perfection V700 Photo (resolution 1200 dpi) and analyzed at the level where the cross-sectional area contained the largest diameter of the tumor, if applicable.

The treatment outcomes were evaluated using the tumor growth inhibition (TGI) index calculated as:

$$\text{TGI index} = \left[1 - \frac{\text{mean area of treated tumors}}{\text{mean area of control tumors}}\right]100\%$$

2.7.2. Evaluation of the intratumoral penetration of fluorescently labeled Dox-PLGA-Cy5.5 nanoparticles by confocal laser scanning microscopy (CLSM)

Preparation of Cy5.5-labeled Dox-PLGA nanoparticles (Dox-PLGA-Cy5.5). For better visualization of the Dox-PLGA nanoparticles by fluorescent microscopy, they were additionally labeled with a fluorescent dye Cyanine 5.5 amine (Cyanine5.5, Cy5.5 analog, amine derivative, Lumiprobe, Germany). The Dox-PLGA-Cy5.5 nanoparticles were prepared, as described by Malinovskaya et al. (2017). Briefly, Cyanine 5.5 amine was covalently linked to a carboxylic terminal group of PLGA (Resomer®502H) via the EDC/NHS coupling reaction. Solutions of Cy5.5 (1 mg [1.5 µmol] in 2 ml of DCM), diisopropylethylamine (0.2 mg [1.53 µmol] in 1 ml of DCM), and EDC (1.9 mg [10 µmol], Sigma, Steinheim, Germany) in 1 ml of DCM were added to a PLGA solution in DCM (600 mg in 5 ml). The reaction mixture was incubated for 48 h under continuous stirring at room temperature. The obtained solution was washed with water to remove excessive reagents and water-soluble by-products, dried over anhydrous sodium sulfate and evaporated. The obtained sediment was dissolved in ethyl acetate and precipitated with hexane (30 ml), followed by filtration and drying to yield the conjugate in the form of light-blue powder. The content of Cy5.5 in the conjugate was measured spectrophotometrically at 684 nm.

The Dox-PLGA-Cy5.5 nanoparticles were produced by a double emulsion solvent evaporation technique as described above using the PLGA-Cy5.5 conjugate with a dye-to-polymer ratio of 1: 600 w/w. The emission spectra were measured over a wavelength range from 550 nm to 650 nm for doxorubicin and 600–700 nm for Cy5.5 amine. The fluorescence measurements were performed at λ_{ex} of 488 nm and 684 nm for doxorubicin and Cy5.5 amine, respectively (spectrofluorimeter Shimadzu RF-6000, Japan).

Evaluation of the intratumoral penetration of Dox-PLGA-Cy5.5 nanoparticles by CLSM. Before administration, the freeze-dried nanoparticles were resuspended in 1% aqueous solution of P188, incubated for 30 min, and then injected i.v. in rats with the 101.8 intracranial glioblastoma on day 14 after tumor implantation. Two hours after administration of the nanoparticles, the rats were deeply anesthetized and perfused transcardially with a 4% p-formaldehyde solution, brains were removed and fixed with 4% p-formaldehyde solution for at least 24 h; then 50 µm-thick brain sections were prepared using a Microme HM 650 V vibratome. Healthy animals were used as control.

Immunohistochemical evaluation. The brain sections were first stained with primary rabbit anti-GFAP (astrocyte marker) and mouse anti-betaIII-tubulin (neuronal marker) antibodies (1:100); then the sections were treated with secondary goat anti-rabbit and anti-mouse antibodies conjugated to Alexa Fluor 488 and Alexa Fluor 594 (1:500), respectively. All antibodies were from Invitrogen, USA. Cell nuclei were counterstained with a Hoechst dye (Invitrogen, USA).

2.8. Statistical analysis

For statistical analysis of the physicochemical data the Student *t*-test was used; statistical significance level was set at p < 0.05. Statistical analysis of the data obtained in the biological experiments was performed with Statsoft Statistica 8.1 (StatSoft Inc., Tulsa, OK, USA) software. The statistically significant differences were evaluated by the non-parametric Mann–Whitney *U* test. Probabilities of p ≤ 0.05 were considered as significant. The data for experimental groups were characterized by the median (Me) and the inter-quartile range (IQR) (L25%; U75%). For the groups with normal distribution the Student *t*-test was used (p < 0.05 and p < 0.01). Results are reported as mean values ± standard deviation (SD).

3. Results and discussion

3.1. Optimization of the nanoparticle preparation process

Composition of external aqueous phase. As mentioned above, our previous studies revealed a high anti-tumor effect of doxorubicin loaded in PLGA nanoparticles (Dox-PLGA) against an experimental rat glioblastoma. Initially, these nanoparticles were prepared by a double emulsion (water-in-oil-in-water) – solvent evaporation technique using PLGA with acid end groups (Resomer® 502H or Lactel®, both with a lactide/glycolide ratio of 50:50 and η ~ 0.21 dL/g) as core polymer and a 1% aqueous solution of polyvinyl alcohol (PVA) with a molecular mass of 30–70 kDa (88% hydrolyzed) as an external phase. This method yielded nanoparticles with parameters acceptable for a proof-of-concept evaluation: a size of ~250 nm, a relatively low PDI of < 0.2, and a doxorubicin loading of 66% or 75% at drug-to-polymer ratios of 1:10 or 1:20, respectively (Gelperina et al., 2010; Wohlfart et al., 2011). However, PVA is not a biodegradable polymer and, therefore, due to toxicological considerations it is not the optimal excipient for injectable formulations. Hence, attempts were made to replace PVA with human serum albumin (HSA) as a safer surfactant. These attempts yielded nanoparticles with a high doxorubicin loading of ~90%. However, the results were not satisfying: the anti-tumor effects were somewhat lower compared to PVA-stabilized nanoparticles and, moreover, employment of HSA led to formation of bigger nanoparticles of ~400 nm with high polydispersity indices of 0.3–0.4 (Gelperina et al., 2010; Wohlfart et al., 2011).

Therefore, one of the primary goals of this study was to optimize the initial Dox-PLGA formulation by selecting a safer stabilizer and by improving the encapsulation efficiency of the nanoparticles.

Polyvinyl alcohol, partially hydrolyzed polyvinyl acetate, is the functional excipient commonly used in PLGA micro- and nanoparticle formulations. As a surfactant it reduces interfacial tension thus increasing the emulsion stability and due to its high affinity to the PLGA particles, it acts as an efficient steric stabilizer that provides stability of the resulting nanosuspension (Birnbaum et al., 2000; Vandervoort and Ludwig, 2002; Sahoo et al., 2002). In general, the stabilizing effect of PVA depends on the degree of hydrolysis and the molecular mass; nevertheless the effective stabilization of emulsions was shown for the PVA with molecular masses in the broad range of 13–180 kDa (Bak and Podgórska, 2013, 2016; Liu et al., 2017).

The pharmaceutical grades of PVA in a similar range (~20–200 kDa, USP 29 Monograph. Polyvinyl alcohol) are used as excipients for many oral and topical medications, which is due to its biocompatibility and low toxicity upon these routes of administration. As a non-biodegradable polymer, PVA, however, is not approved as an excipient for injectable formulations. At the same time, accumulation of PVA with molecular masses in the range of 15–200 kDa in the rat organs upon intravenous injection was shown to be rather low, and its interaction with the the cells is insignificant (Kaneo et al., 2005; Yamaoka et al., 1995). At the same, the profile of the biodistribution, as well as the pharmacokinetic parameters of PVA upon intravenous administration,

strongly depend on the molecular mass. Thus the mean half-life times in the blood of mice and the rate of urinary excretion 1 h after intravenous injection ranged from 52 min and > 80% for PVA 15 kDa to 684 min and < 30% for PVA 70 kDa, respectively. PVA 15 kDa also showed only minor accumulation in the liver and internalization into the cells. The cut-off for the glomerular permeability of PVA was reported to be 30 kDa (Yamaoka et al., 1995; Tabata et al., 1998).

Based on the aforementioned favorable properties, the low molecular mass PVA appeared to be a suitable nanoparticle stabilizer. Moreover, as mentioned above, the surface activity and stabilizing effect of PVA depend on its molecular structure, i.e. on molecular mass and content of residual acetate groups. However, as observed by Murakami et al. (1997), the degree of PVA hydrolysis plays a more important role in the process of the nanoparticle formation than its molecular mass with lower hydrolyzed grades (< 90%) resulting in better stabilizing effects. Therefore, more specifically, PVA with molecular mass of 9–10 kDa, 80% hydrolyzed (Sigma, Steinheim, Germany) was considered to be the most suitable candidate among other low molecular mass PVA grades and hence was chosen as stabilizer for the doxorubicin-loaded PLGA nanoparticles.

Further, a key factor for achieving a high loading of doxorubicin in the nanoparticles is its effective partition from the aqueous phase to the organic phase. Doxorubicin hydrochloride is readily soluble in water with log P of 1.27 in a 1-octanol/water system. However, the presence of the primary amine group in the glycosidic fragment with the pKa value of 8.22 (Vigevani and Williamson, 1981), enables the regulation of doxorubicin hydrophilicity, and, therefore, its partition between the hydrophilic (aqueous) and hydrophobic (organic) phases by adjusting the pH level. This approach has already been applied by other authors who used triethylamine (Kataoka et al. 2000) or a strong basic buffer (Sanson et al., 2010) to decrease aqueous solubility of doxorubicin and improve its loading in the polymeric micelles or vesicles. Since the stability of doxorubicin at basic pH is impaired (Janssen et al., 1985; Beijnen et al., 1986), in the present study a PVA (9–10 kDa) solution in phosphate buffer saline (PBS pH 7.4) was used as an external aqueous phase. As shown in Table 1, this approach allowed an increase in the encapsulation efficiency of the Dox-PLGA nanoparticles from 66% to > 85% at a drug-to-polymer ratio of 1:10. Accordingly, when PVA solutions in PBS with pH 6 or in water were used, the encapsulation efficiency dropped to 70% and ~50%, respectively. Obviously, in PBS the presence of phosphate ions enhances the loading of doxorubicin in the nanoparticles due to formation of doxorubicin phosphate which has a solubility of ~0.1 mg/ml (Alyane et al., 2016). The stability of doxorubicin during the above preparation procedure was confirmed using HPLC. The content of doxorubicin was found to be 98.98% and 99.10% for the doxorubicin-loaded PLGA NP and the free doxorubicin, respectively.

In accordance with this explanation, comparison of the kinetics of the doxorubicin release from the PLGA NPs, obtained using solutions of 1% PVA 9–10 kDa in PBS (Dox-PLGA-PBS) or in distilled water (Dox-PLGA) demonstrated a longer retention of the less soluble doxorubicin phosphate in the Dox-PLGA-PBS nanoparticles. Indeed, although both formulations displayed biphasic release profiles that are typical for drugs entrapped in nanoparticles, the Dox-PLGA formulation released ~70% of doxorubicin within the first 6 h (Gelperina et al., 2010), whereas the amount of doxorubicin released from the Dox-PLGA-PBS nanoparticles reached only 40% within the same period of time (Fig. 1).

Predictably, the size and polydispersity of the nanoparticles were influenced by the homogenization conditions of the secondary emulsion depending on the type of the homogenizer (Table 1): a Microfluidizer® (M-110P) produced a more homogeneous nanoparticle suspension as compared to a valve type homogenizer PandaPLUS at the same homogenization pressure and processing time (1000 bar, 5 min). The average particle sizes were 111 ± 4 nm (PDI 0.135 ± 0.025) and 150 ± 27 nm (PDI 0.175 ± 0.021) for M-110P and PandaPLUS, respectively. This phenomenon, observed also by other authors (Lee and

Table 1
Influence of the technological parameters on nanoparticle encapsulation efficiency and size distribution (Dox/PLGA = 1:10, w/w; homogenization: 1000 bar/5 min; representative data).

No	External aqueous phase		EE, %	Homogenizer	Average diameter, nm	PDI
	Composition	pH				
1[#]	1% PVA 30–70 kDa in water	5.8	66	EmulsiFlex C5/ 600 bar	253 ± 3	0.179
2[*]	1% PVA 9–10 kDa in PBS	7.4	85 ± 5	Panda	151 ± 27	0.175 ± 0.021
3	1% PVA 9–10 kDa in PBS	6.0	71	Panda	145	0.163
4	1% PVA 9–10 kDa in water	5.7	53	Panda	121	0.125
5[**]	1% PVA 9–10 kDa in PBS	7.4	90 ± 2	M-110P	118 ± 4	0.135 ± 0.025
6	1% PVA 9–10 kDa in PB	7.4	82	M-110P	109	0.128
7	1% PVA 9–10 kDa in PBS	6.0	68	M-110P	131	0.243
8	1% PVA 9–10 kDa in water	5.7	34	M-110P	102	0.132

[#] Data from Wohlfart et al. (2011).

[*] n = 4.

[**] n = 5.

Norton, 2013; Mao et al., 2010), may be attributed to a narrower distribution of shear forces and a better temperature control provided by the Microfluidizer® system as compared to the valve homogenizer, which resulted in a decreased coalescence of the droplets in the emulsion and formation of smaller particles with a lower PDI. A considerably bigger size of the nanoparticles produced with EmulsiFlex® C5 (Avestin, Ottawa, Canada) is most probably explained by the lower homogenization pressure (600 bar vs 1000 bar) applied in this experiment, a factor that is also known to influence the particle size and PDI (Lee and Norton, 2013).

Influence of PVA structure. The correctness of the surfactant choice was confirmed by comparison of different commercial grades of PVA. In order to get an insight into the influence of the PVA molecular mass and degree of hydrolysis on nanoparticle size and drug loading the Dox-PLGA, NPs were manufactured using different commercial grades of PVA, including a pharmaceutical grade PVA Mowiol® 3–96 (MM ~ 13 kDa, degree of hydrolysis 96%, Kuraray Europe GmbH, Germany). The representative physicochemical parameters of the nanoparticles obtained using different PVA grades are shown in Table 2.

The degree of PVA hydrolysis appeared to be more important for controlling the size and polydispersity of the Dox-PLGA nanoparticles than molecular mass, which correlates with the data of Murakami et al. (1997). Indeed, among three low-molecular types only the PVA with a 80% degree of hydrolysis enabled the preparation of the nanoparticles with a size of ~130 nm. Preparation of the nanoparticles using low molecular weight PVA with a higher degree of hydrolysis (80–100%) resulted in an increase in the nanoparticle size (up to 1 μm). Although the obtained nanosuspension initially remained homogeneous, after

lyophilization the particle size increased, and the suspension lost its homogeneity. The same phenomenon also was observed by Murakami et al. (1997) who suggested that the residual acetate groups of low-hydrolyzed PVA prevent hydrogen bond formation between hydroxyl groups of free PVA in solution and the residual PVA molecules that remain associated with the nanoparticle surface, which hinders their aggregation. Accordingly, when the degree of hydrolysis PVA is high, the hydrocarbon chains formed during freeze-drying hinder the formation of the hydrated layer around NPs leading to NP aggregation and low resuspendability (Sahoo et al., 2002). A slight decrease of the nanoparticle size along with the decrease of the molecular masses observed for the PVA types with similar degrees of hydrolysis of 80–88% and different molecular masses of 9–10 kDa or 30–70 kDa (133 nm and 170 nm, respectively) correlated with a comparatively lower surface tension produced by low molecular PVA (Tables 2 and 3).

The concentrations of the components in the model system used for the measurements of the interfacial tension were similar to those used for the nanoparticle preparation, i.e. 16.7% PLGA solution in dichloromethane and 0.2% or 1.0% doxorubicin solution in 1% PVA. As shown in Table 3, the interfacial tension values depended on the molecular properties of PVA. Higher interfacial tension value correlated with a larger size of the obtained nanoparticles. Interestingly, the increase of the doxorubicin concentration in the system also led to the increase of the surface tension.
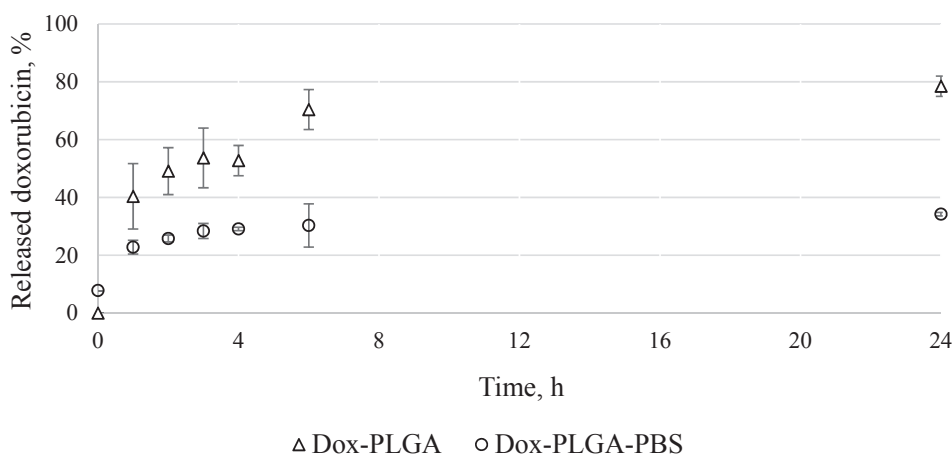

Fig. 1. Kinetics of doxorubicin release from the PLGA nanoparticles prepared using 1% PVA 9–10 kDa solutions either in water [Dox-PLGA] or in PBS [Dox-PLGA-PBS] as external phases (Dox: PLGA ratio = 1:10 w/w; release medium 0.9% NaCl solution; 37 °C, 25-fold dilution; n = 3, P = 0.95).

Table 2

Influence of PVA properties on the particle size and encapsulation efficiency of Dox-PLGA nanoparticles. External phase: 1% PVA in PBS (pH 7.4), Dox:PLGA = 1:10 w/w, homogenizer PandaPLUS 2000, pressure 1000 bar (representative data).

PVA properties[#]		EE, %	Particle size and size distribution			
			Before freeze-drying		After freeze-drying	
MM, kDa	Degree of hydrolysis, %		Average size, nm	PDI	Average size, nm	PDI
9–10	80	86	132 ± 0	0.157 ± 0.013	133 ± 1	0.163 ± 0.016
30–70	88	68	154 ± 16	0.143 ± 0.014	173 ± 0	0.115 ± 0.011
~13	96	66	1516 ± 87	0.842 ± 0.011	4614 ± 713	0.617 ± 0.245
~15	100	42	2403 ± 439	0.620 ± 0.093	4448 ± 696	0.727 ± 0.433

[#] Manufacturers' data.

Table 3

Interfacial tension values (σ, mN/m) in a liquid-liquid heterophase system consisting of a 16.7% PLGA solution in dichloromethane and a doxorubicin solution in 1% PVA solution in PBS pH7.4 (25° C, representative values).

PVA grades		σ, mN/m	
MM, kDa	Degree of hydrolysis, %	C_{dox} = 0.2%	C_{dox} = 1.0%
9–10	80	3.07	3.57
30–70	87–90	4.60	6.07
~13	96	7.38	9.85
~15	100	8.62	8.96

3.2. Evaluation of irradiation stability of doxorubicin-loaded PLGA nanoparticles

The Dox-PLGA formulation was intended for the intravenous administration, and, therefore, it required sterilization. Gamma sterilization is a cost-effective pharmacopoeia method to attain terminal sterilization with a high level of sterility assurance while avoiding undesirable heating of the product or employment of toxic chemicals. Polylactides are moisture- and heat-sensitive polymers, and thus the PLGA-based formulations represent good candidates for radiation sterilization (Athanasiou et al., 1996; Sintzel et al., 1997). At the same time, it is generally known that ionising radiation may considerably damage molecular structure of polylactides inducing cross-linking or destruction of the polymeric chains in a dose-dependent manner (Williams et al., 2006; Loo et al., 2004). The radiation effects and especially formation of reactive radicals may also impair the stability of the encapsulated drug and changes in its release profile from the PLA or PLGA particles. Overall, these observations suggest that stability of the nanoparticle-based formulation upon gamma sterilization depends on the irradiation dose as well as on the physicochemical characteristics of the drug, its interaction with the microenvironment (i.e. polymeric core and excipients), drug loading, etc. (Volland et al., 1994; Bittner et al., 1999; Caliş et al., 2002; Montanari et al., 2001). Therefore, although the doxorubicin substance exhibited a good stability upon irradiation in the solid state (Varshney and Dodke, 2004; Kaczmarek et al. 2013), the feasibility of irradiation sterilization of the Dox-PLGA formulation required investigation.

Hence, in the present study the feasibility of the Dox-PLGA NP sterilization by irradiation was evaluated using either gamma irradiation or electron beam irradiation. These processes are characterized by different time and intensity scales: gamma irradiation is highly penetrating with a low dose rate, whereas e-beam irradiation is characterized by a lower penetration but a significantly higher dose rate. Accordingly, the dose rates used in the present study were 2 Gy/s and 1.6×10^3 Gy/s, respectively. The influence of irradiation on the physicochemical parameters, such as the mean particle size and size distribution, doxorubicin content and stability as well as the drug release profile was investigated at three dose levels of 10, 15, and 25 kGy. For evaluation of the role of the doxorubicin content in the nanoparticles, the Dox-PLGA nanoparticles with the drug-to-polymer ratios of 1:10 [Dox-PLGA (1:10)] and 1:20 [Dox-PLGA (1:20)] as well as unloaded nanoparticles (PLGA-Placebo) were used in these experiments.

Influence on the nanoparticle size. Measurements of the mean particle size and size distribution by DLS demonstrated that the applied doses of electron beam irradiation (up to 25 kGy) did not significantly alter the mean particle size of both, PLGA-Placebo and Dox-PLGA nanoparticles (Table 4). Gamma irradiation at the doses of 10 and 15 kGy induced a slight increase in mean particle size and polydispersity index. The dose of 25 kGy resulted in the significant increase of the mean particle size

Table 4

Influence of the type and dose of irradiation on the size and polydispersity index of doxorubicin-loaded PLGA nanoparticles.

Dose of irradiation (kGy)	Dox-PLGA (1:10)			Dox-PLGA (1:20)		
	Mean size, nm	PDI	Volume size distribution, nm (%)	Mean size, nm	PDI	Volume size distribution, nm (%)
Before irradiation	121 ± 1	0.125 ± 0.011	116 (100)	127 ± 16	0.142 ± 0.012	121 (100)
Electron beam irradiation						
10	121 ± 1	0.132 ± 0.017	120 (100)	132 ± 1	0.146 ± 0.014	130 (100)
15	1218 ± 1	0.129 ± 0.014	114 (100)	124 ± 0	0.150 ± 0.006	119 (100)
25	119 ± 1	0.133 ± 0.012	113 (100)	126 ± 1	0.169 ± 0.012	120 (99) 5161 (1)
Gamma irradiation						
10	123 ± 1	0.148 ± 0.012	116 (1 0 0)	124 ± 1	0.149 ± 0.010	116 (100) 5242 (1)
15	138 ± 2	0.573 ± 0.072	590 (65) 132 (28) 2719 (0.1)	128 ± 04	0.187 ± 0.359	116.6 (100) 5096 (4)
25	121 ± 1	121.00 ± 0.70	114 (1 0 0)	564 ± 263	0.818 ± 0.048	16 (7) 137 (14) 3210 (79)

Table 5
Content of doxorubicin and maximal individual impurity after irradiation of the Dox-PLGA formulations (representative results).

Formulation	Substance	Content, %						
		Before irradiation	Electron beam irradiation, kGy			Gamma-irradiation, kGy		
			10	15	25	10	15	25
Dox-PLGA (1:10)	Doxorubicin	98.98	97.91	98.89	97.59	96.97	96.68	95.06
	Maximum individual impurity	0.64	0.45	0.49	1.0	1.35	1.18	1.77
Dox-PLGA (1:20)	Doxorubicin	99.11	98.37	98.81	97.94	96.37	95.91	94.39
	Maximum individual impurity	0.38	0.55	0.43	0.64	0.86	0.97	1.40

and the formation of a larger microparticle fraction for both types of the Dox-PLGA nanoparticles (1:10 and 1:20). Nevertheless, all sterilized samples could be easily resuspended in water.

Influence on doxorubicin stability. The influence of electron beam irradiation and gamma irradiation on the stability of doxorubicin loaded in PLGA NPs was evaluated by HPLC. Amounts of the doxorubicin-related degradation products in the samples were below 5% for all irradiation regimens with the exception of the samples subjected to gamma-irradiation at the dose of 25 kGy, where it reached ~5% (Table 5).

The amount of doxorubicin degradation products showed a tendency to increase with the irradiation dose, which was more noticeable for the samples subjected to gamma irradiation. As mentioned above, the energy of gamma irradiation is lower. Thus, it takes more time to reach the same dose values compared to electron beam irradiation where the higher dose rate produced by e-beams requires a shorter exposure time and thus induced less damage.

The obtained results, therefore, indicate that the irradiation of the Dox-PLGA nanoparticles led to formation of the doxorubicin degradation products, and the amount of which was increasing in parallel with the increase of the irradiation dose and was higher in the gamma-irradiated samples.

Influence on polymer stability (molecular mass distribution of PLGA). The influence of ionizing irradiation on the molecular mass distribution of PLGA before and after sterilization was assessed by gel-permeation chromatography (GPC). The effect of irradiation (gamma and beta irradiation to the doses of 10, 15, and 25 kGy) was evaluated for empty PLGA-Placebo and doxorubicin-loaded PLGA nanoparticles (Dox:PLGA = 1:10 or 1:20, w/w). All nanoparticle formulations were produced using Resomer® 502H, 1% PVA 9–10 kDa as the stabilizer and 5% mannitol as cryoprotectant. As shown in Table 6, both, the weight average molecular weight (Mw) and the number average molecular weight of PLGA, were found to somewhat decrease after sterilization which could be explained by polymer chain scission induced by

irradiation. This finding correlates with the results of other authors (Fernández-Carballido et al., 2004; Bittner et al 1999; Caliş et al., 2002).

It is noteworthy that the level of PLGA degradation tended to decrease along with an increase in the doxorubicin content in the formulation. This observation is in accordance with the results of our previous studies that demonstrated the contribution of doxorubicin to the radiolytic stability of the poly(butyl cyanoacrylate) nanoparticles (Maksimenko et al., 2008). This phenomenon was due to a considerably decreased concentration of the stable radicals in the irradiated nanoparticles in the presence of doxorubicin. A similar protecting effect of the encapsulated drug on the polymeric matrix was observed also for clonazepam-loaded PLGA microspheres subjected to gamma-irradiation (Montanari et al., 2001). Interestingly, there was no significant difference between the influence of electron beam- and gamma irradiation on the properties of PLGA.

Influence on drug release profile. Despite the slight decrease in the molecular weight of the polymer, both, electron-beam and gamma irradiation of the samples up to the dose of 15 kGy, did not significantly influence the release profile of doxorubicin. Significant changes in the release rate were only observed for the samples sterilized with gamma irradiation at the dose of 25 kGy (data not shown).

The obtained results demonstrated that the straightforward electron beam irradiation of the Dox-PLGA nanoparticles up to the dose of 15 kGy did not significantly alter the formulation parameters; gamma irradiation at this dose level was less sparing. Higher doses of both, e-beam and gamma irradiation, induced considerable changes of all nanoparticle parameters including the increase in the impurity levels. Taken together with the observation that the amount of doxorubicin degradation products increased upon storage (Kaushik and Bansal, 2015; Cielecka-Piontek et al., 2009) and that the storage stability of irradiated polymers can be impaired (Dorati et al., 2008), these results indicate that the process of the terminal sterilization of the Dox-PLGA formulation requires further optimization.
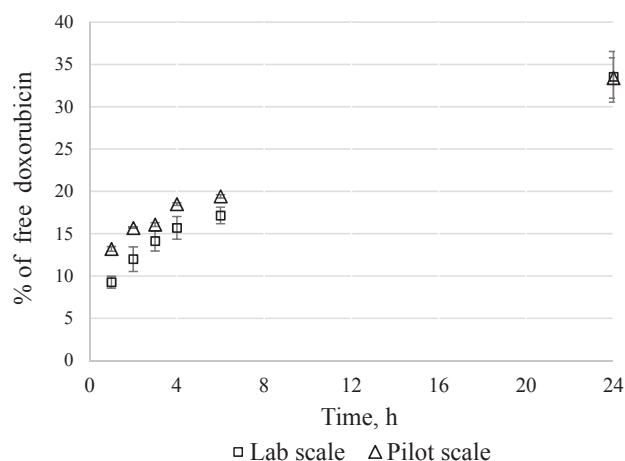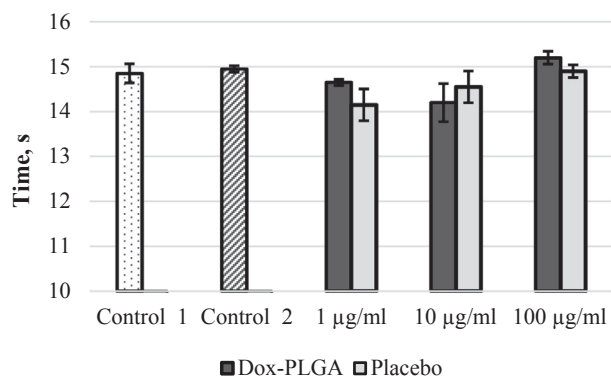
3.3. Preparation of the pilot batch

Scaling-up of the manufacturing process to a pilot scale was performed with a batch size increase from 120 ml to 1500 ml. Similarly to laboratory batches, pilot batches were produced by a double emulsification – solvent evaporation technique. An M-110 Microfluidizer® was used for the final homogenization step; however, in this case the homogenization time was prolonged to 30 min (3-min homogenization was applied for the laboratory batches). The composition of the external aqueous phase used in the scaled-up process was slightly modified: 1% PVA 9–10 kDa solution in 0.01 M phosphate buffer (PB: 8 mM Na_2HPO_4, 2 mM KH_2PO_4, pH 7.4) was used instead of its solution in 0.01 M PBS. This alteration did not influence the nanoparticle parameters (data not shown).

The scaled-up process was highly reproducible: only minor interbatch variations of all parameters were observed for five parallel batches (Table 7). The nanoparticle encapsulation efficiency and the yield of doxorubicin obtained in both processes were similar. However, the
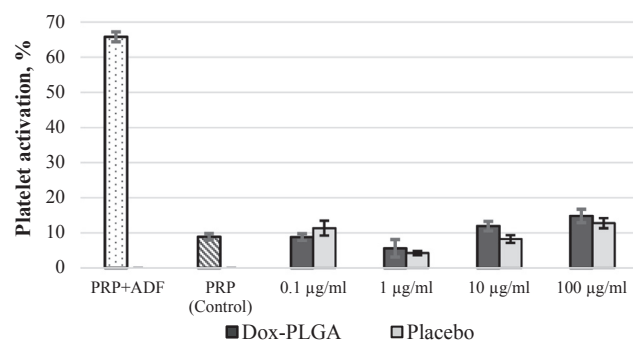
Table 6
Influence of irradiation on the molecular mass distribution of PLGA polymer in non-loaded and doxorubicin-loaded PLGA nanoparticles.

Dose of irradiation, kGy	Molecular mass, Da					
	PLGA-Placebo		Dox-PLGA (1:20 w/w)		Dox-PLGA (1:10 w/w)	
	Mn	Mw	Mn	Mw	Mn	Mw
Control	8400	14,070	9494	14,395	10,020	14,800
Electron beam irradiation						
10	8500	14,500	9150	13,770	9630	14,070
15	7700	12,900	9040	13,460	9400	13,660
25	7290	12,220	8830	13,220	9500	14,030
Gamma-irradiation						
10	7080	11,800	8500	12,590	9430	14,000
15	7440	12,360	9380	14,000	9425	13,970
25	7250	12,020	8940	13,300	9250	13,700

Table 7

Physicochemical properties of Dox-PLGA nanoparticles produced on laboratory and pilot scales (n = 5).

Batch	External aqueous phase			Before centrifugation		After centrifugation		Zeta potential, mV	EE, %	Yield*, %
	Composi-tion	pH	Batch volume, ml	Average diameter, nm	PDI	Average diameter, nm	PDI			
Lab scale Dox-PLGA-l.s.	1% PVA 9–10 kDa in PBS	7.4	60	111 ± 4	0.135 ± 0.025	–	–	−10.1 ± 1.1	90 ± 2	69 ± 2
Pilot scale Dox-PLGA-p.s.	1% PVA 9–10 kDa in PB	7.4	1500	137 ± 14	0.244 ± 0.062	108 ± 6	0.056 ± 0.010	−11.1 ± 0.9	90 ± 2	70 ± 4

* as doxorubicin.

Fig. 2. Kinetics of doxorubicin release from the Dox-PLGA nanoparticles produced in the laboratory or the pilot scale (representative batches; release medium 1% poloxamer 188 solution; 37 °C, 25-fold dilution; n = 3, p = 0.95).

Fig. 3. Coagulation time (PT) as a function of nanoparticle type and concentration. Controls 1 and 2 – coagulation times of blood samples immediately and 30 min after withdrawal, respectively (mean values ± SD; n = 3).

size and polydispersity of the nanoparticles produced by the pilot-scale process (Dox-PLGA-p.s.) were slightly higher as compared to the laboratory batches (Dox-PLGA-l.s.): 137 ± 14 nm (PDI 0.244 ± 0.062) versus 111 ± 4 nm (PDI 0.135 ± 0.025), respectively.

To further reduce the polydispersity of the particles the nanosuspension was additionally subjected to continuous high-speed flow centrifugation. The centrifugation step led to a considerable reduction of the mean nanoparticle size and polydispersity to 108 ± 6 nm and 0.056 ± 0.010, respectively (Table 7). This small size and the low polydispersity enabled the sterile filtration with a 0.22 μm pore size membrane filter. Measurements of the particle size after the sterilizing filtration did not reveal any significant change in particle size and size distribution. No filter clogging or significant loss of material by adsorption on the membrane surface did occur (data not shown). The

Fig. 4. Platelet activation (level of P-selectin expression) after incubation of platelet-rich plasma (PRP) with PLGA-Dox and Placebo nanoparticles. PRP – negative control; PRP + ADP (platelet aggregation inductor adenosine diphosphate) – positive control (mean values ± SD; n = 3).

Table 8

Hemolysis (%) after incubation of blood with Dox-PLGA and PLGA-Placebo nanoparticles (representative data).

Sample	Concentration, μg/ml	Hemolysis, %
PLGA-Placebo	1	0.175
	10	0.53
	100	1.23
Dox-PLGA	1	0.7
	10	1.75
	100	7.29

Table 9

Quantitative analysis of tumor incidence and tumor size after chemotherapy of 101.8 rat glioblastoma with different formulations of doxorubicin.

Treatment regimen: 3 × 1.5 mg/kg, day 14			
Groups	Tumor incidence	Tumor area: Me (min, max), mm^2	TGI index, %
Control untreated	10/10	19,2 (13.6; 22.1)	–
Free doxorubicin	10/10	5.8 (3.25; 7.0)	70
Dox-PLGA-p.s. + P188	11/11	0.7(0.1; 5.9)	97

sterility testing performed according to pharmacopoeia requirements confirmed the validity of the sterilization process (data not shown).

Profiles of the doxorubicin release from the lab scale Dox-PLGA-l.s. and the pilot scale Dox-PLGA-p.s. nanoparticles were similar (Fig. 2). Continuous incubation of the Dox-PLGA nanoparticles in the media simulating the physiological conditions such as PBS and 0.9% NaCl was associated with precipitation, which could be due to the known impairment of colloidal stability of the nanoparticles in the presence of electrolytes; precipitation of doxorubicin phosphate might also occur in the presence of phosphate ions. For this reason, in the continuous experiment a 1% poloxamer 188 solution was used as release medium. Although these experimental conditions did not simulate the
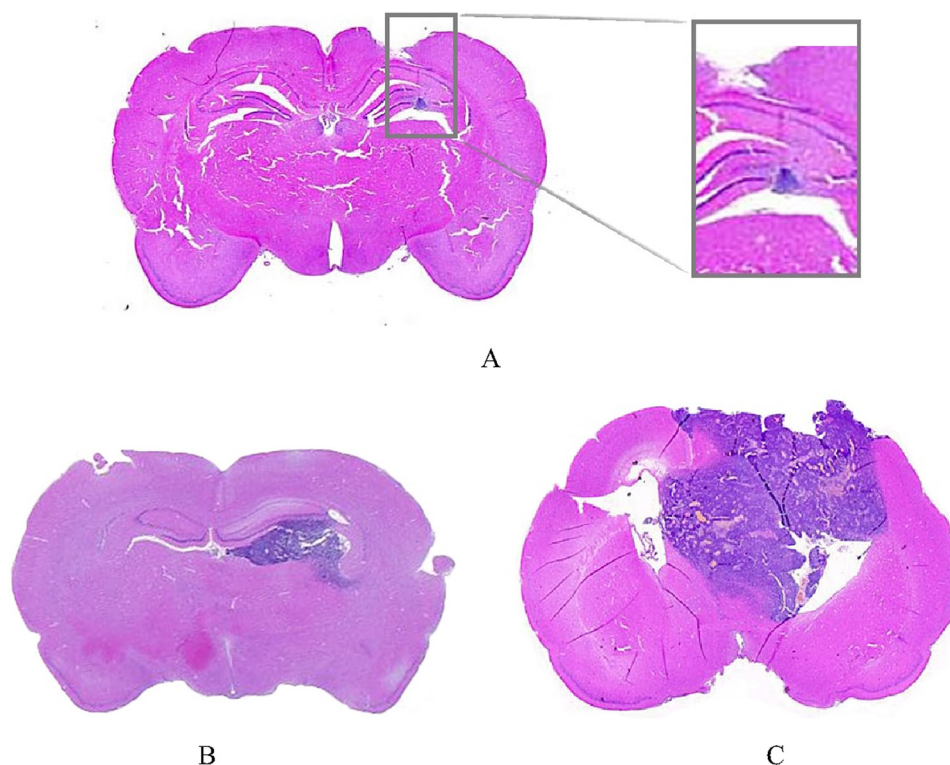
Fig. 5. Representative brain sections of Wistar rats with the intracranially implanted 101.8 glioblastoma on day 14 post tumor implantation (stained with haematoxylin & eosin): A - doxorubicin loaded in PLGA nanoparticles coated with poloxamer 188 (Dox-PLGA-p.s.), inset magnification ×10; B – free doxorubicin (both injected i.v. in the dose of 3×1.5 mg/kg on days 2, 5 and 8 post tumor implantation); C - untreated control.
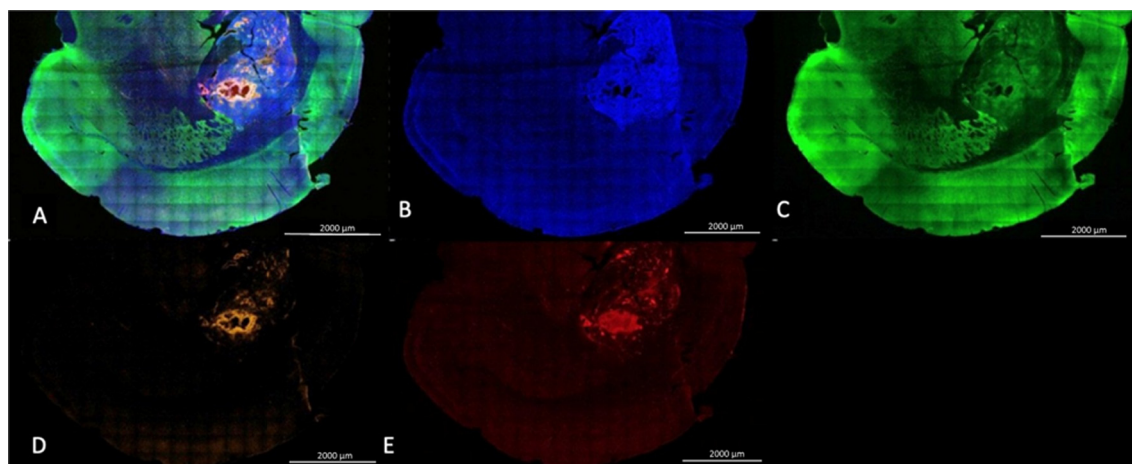

Fig. 6. Brain sections of Wistar rats with the intracranially implanted 101.8 glioblastoma 2 h post intravenous administration of Dox-PLGA-Cy5.5 nanoparticles (SLCM): A - merged image; B – fluorescence of cell nuclei (Hoechst staining); hypercellular tumor regions are noted by intense Hoechst staining; C – beta-III-tubulin positive neurons; D – doxorubicin fluorescence; E – Cy5.5 fluorescence. Scale bar = 2000 μm.

physiological conditions, they helped to avoid formation of precipitate during incubation and enabled a reliable comparison of the release profiles of the samples.

3.4. Evaluation of hemocompatibility of Dox-PLGA nanoparticles

Interaction of the PLGA-Dox-p.s nanoparticles with blood components was investigated by generally accepted tests such as the blood coagulation test, hemolysis and platelet aggregation studies, and nanoparticle-protein interaction assays (Neun and Dobrovolskaia, 2011; Fornaguera and Solans, 2017; Cho et al., 2013). Non-loaded nanoparticles (PLGA-Placebo) with similar parameters were used as control.

As shown in Fig. 3, the PLGA-Dox as well as the PLGA-Placebo nanoparticles did not influence the blood coagulation time at concentrations up to 100 μg/ml: the PT values remained within the physiological range of 12–15 s (normal physiological values) for all tested samples, and there was no statistically significant difference between the control and experimental groups.

The ability of the nanoparticles to induce platelet activation was evaluated by measuring the level of P-selectin expression on the surface of activated platelets by flow cytometry. Platelet-rich plasma (PRP) incubated with the platelet aggregation inductor (platelet aggregation inductor adenosine diphosphate, ADP) was used as a positive control. As shown in Fig. 4, incubation of PRP with the nanoparticles did not induce platelet activation in concentrations up to 10 μg/ml. A slight increase in the number of activated platelets (~5% compared to negative control) was observed for both, doxorubicin-loaded and Placebo PLGA nanoparticles only at the concentration of 100 μg/ml. However, this concentration considerably exceeded the projected blood levels after intravenous administration of therapeutic doses (50–70 mg/m^2) of
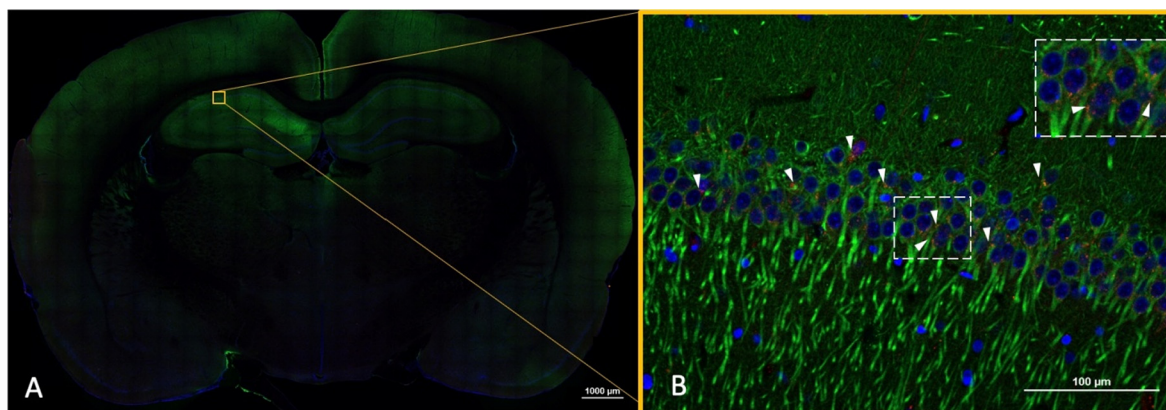
Fig. 7. Accumulation of Dox-PLGA-Cy5.5 nanoparticles in hippocampal neurons (healthy Wistar rats, 2 h post intravenous administration of Dox-PLGA-Cy5.5 nanoparticles). A – Large merged image; B – Uptake of nanoparticles in hippocampal neurons. Blue – fluorescence of cell nuclei (Hoechst staining); green – GFAP-positive astrocytes; red – Dox-PLGA-Cy5.5 nanoparticles (arrows). Scale bars: 1000 µm (A), 100 µm (B), 50 µm (high magnification panel). (For interpretation of the references to color in this figure legend, the reader is referred to the web version of this article.)

the doxorubicin formulations.

The percentage of hemolysis after incubation of blood samples with the doxorubicin-loaded and placebo nanoparticles was evaluated at different concentrations. Neither of the nanoparticle samples produced hemolysis after 3 h of incubation: the percentage of hemolysis was between 0.1 and 1.8 % compared to control (Table 8). A slight increase was observed for the Dox-PLGA nanoparticles at the concentration of 100 µg/ml (hemolysis 7.29%), which probably could be attributed to the erythrocyte membrane damage by released doxorubicin (Marczak et al., 2006).

The study of the nanoparticle hemocompatibility confirmed the safety of the Dox-PLGA formulation: the nanoparticles did not produce any influence on the blood coagulation system (coagulation time, platelet activation) and did not induce hemolysis at concentrations relevant for the clinical application.

3.5. Evaluation of the anti-tumor effect in the orthotopic 101.8 glioblastoma model

The orthotopic 101.8 rat glioblastoma previously was used for the evaluation of the anti-tumor efficacy of the nanoparticle-based doxorubicin formulations and appeared to be a reliable and reproducible brain tumor model (Steiniger et al., 2004; Ambruosi et al., 2006; Gelperina et al., 2010). Moreover, this tumor model is characterized by fast proliferation and an invasive growth pattern (Hekmatara et al., 2009; Wohlfart et al., 2011), and in this way it is similar to human grade IV glioblastomas.

The objective of the present experiment was to evaluate the anti-tumor effect of the optimized Dox-PLGA nanoparticles produced in the pilot scale (Dox-PLGA-p.s). The efficacy of the treatment regimen (3 × 1.5 mg/kg on days 2, 5, and 8 post tumor implantation) was verified in a number of previous studies cited above. In order to enable a comparison of the results, this treatment regimen also was employed in the present study. A higher efficacy of the P188-coated Dox-PLGA nanoparticles compared to non-coated nanoparticles was already shown previously in the same tumor model (Gelperina et al., 2010; Wohlfart et al., 2011). Consequently, in order to spare animals, the non-coated nanoparticles were not tested in this experiment. Untreated animals and animals treated with free doxorubicin in solution were used as controls. The results were assessed by histology on day 14 post tumor implantation. For the evaluation of the tumor size the maximal tumor area was measured in haematoxylin-eosin-stained brain sections of each animal. The Dox-PLGA-p.s. nanoparticles used in this experiment had the following physicochemical parameters: encapsulation efficiency 91%; mean diameter 107 nm; PDI 0.059 ± 0.005; zeta potential −11.1 mV.

Table 9 shows the mean as well as the smallest and the largest tumor sizes and the tumor growth inhibition (TGI) indices obtained after treatment of glioblastoma 101.8 using the new formulation Dox-PLGA-p.s. This formulation exhibited a considerable inhibition of tumor growth with a TGI index of 97%; the TGI index of doxorubicin was lower, i.e. 70%. It is noteworthy that in the group treated with the Dox-PLGA-p.s formulation 4/11 animals had only micro-tumors with sizes of < 0.1 mm. The anti-tumor effect of the free doxorubicin in a 101.8 glioblastoma model also was observed in previous studies using the same experimental modalities (Steiniger et al., 2004; Gelperina et al., 2010; Hekmatara et al., 2009). This effect most probably can be explained by an enhanced delivery of the free doxorubicin to the tumor that was enabled by the partial disruption of the BBB caused by the tumor growth (i.e. on days 5 and 8 post tumor implantation). The representative images of the brain sections with 101.8 glioblastoma obtained from the animals treated with Dox-PLGA-p.s. + P188 or Dox as well as from the control group are shown in Fig. 5A–C.

The lower anti-tumor effects of both, Dox and Dox-PLGA, observed in the study of Wohlfart et al. (2011) as compared to the present experiment (32% and 67% versus 70% and 97%, respectively) could be explained by the later time of the tumor size measurement, i.e. the longer time interval between the end of the treatment course and the day of measurement, which may indicate a tendency for the recurrence of the tumor growth after discontinuation of the therapy. However, both experiments revealed the considerable advantage of the Dox-PLGA formulation over free doxorubicin. This is an important observation because the optimized procedure have modified the nanoparticle parameters considered to be essential for their in vivo performance, i.e. the encapsulation efficiency increased from 66% to > 90% and the nanoparticle size was reduced from 250 nm to 110 nm.

The final Dox-PLGA-p.s. formulation contained mannitol (Dox-mannitol ratio was ~1:33, w/w). Therefore, the animals received intravenously 1.5 mg/kg of doxorubicin and ~50 mg/kg of mannitol as a single dose. Mannitol is a well-known hyperosmotic agent used for the management of cerebral edema and for enhanced delivery of the chemotherapeutics to the brain due to the transient BBB disruption (BBBD) following intraarterial administration (Riina et al., 2009; Esquenazi et al., 2017). In humans, the effective doses of intraarterial mannitol (20–25% solutions) range from 0.5 to 1.5 g/kg. Intravenous administration of mannitol also is used to decrease the intracranial pressure by osmotic withdrawal of excessive fluid from the brain. However, as shown by Chen et al. (2013), mannitol injected intravenously in rats did not increase the BBB permeability for large (Evans blue complex with serum albumin) and small (NaF) molecules even in the dose of 0.5 g/kg.
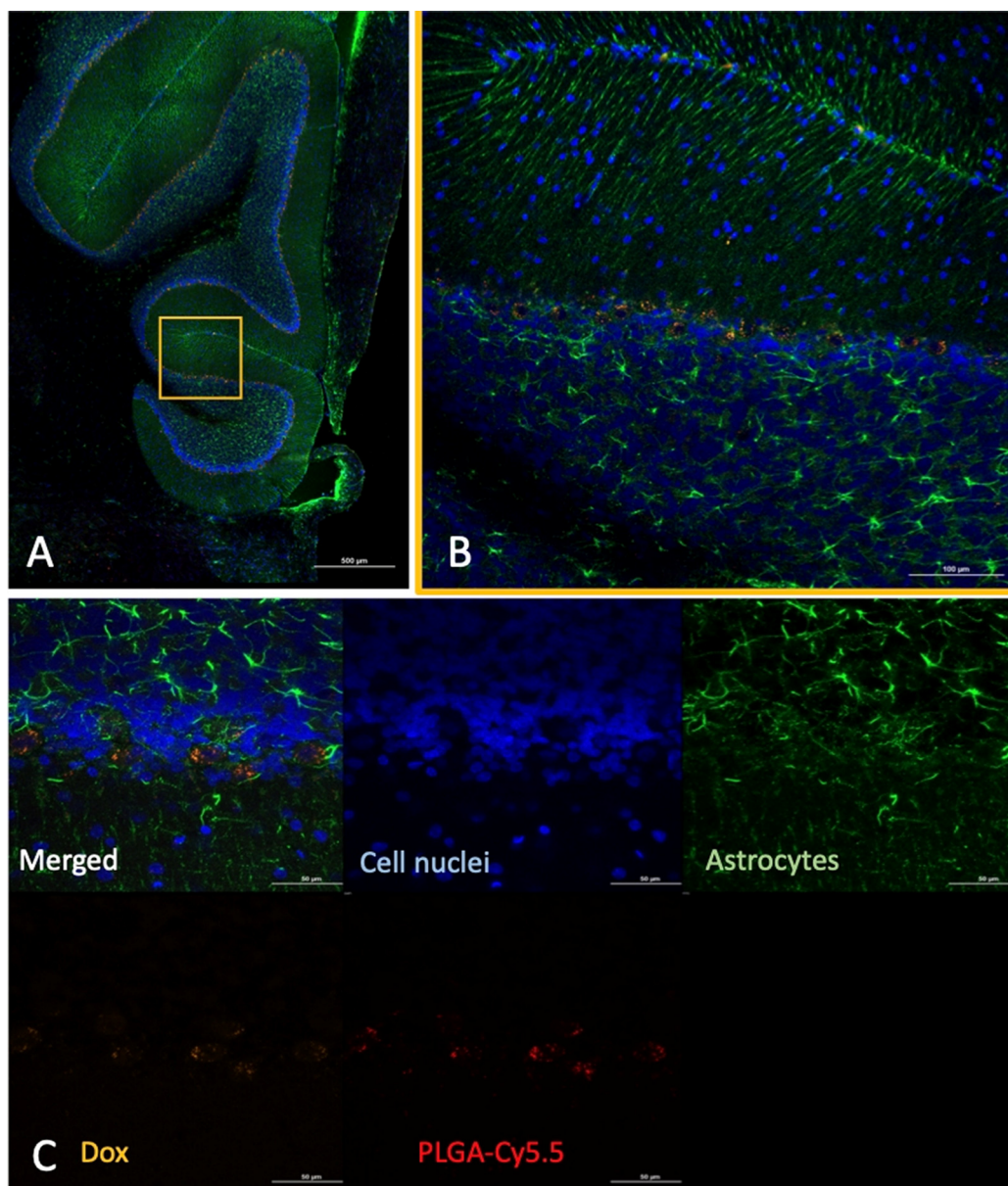
Fig. 8. Accumulation of Dox-PLGA-Cy5.5 nanoparticles in Purkinje cells (healthy Wistar rats, 2 h post intravenous administration of Dox-PLGA-Cy5.5 nanoparticles). A – large merged image; B – nanoparticle uptake in Purkinje cells; C – maximal intensity projection (Z-stacks), depth 10 μm. Blue – fluorescence of cell nuclei (Hoechst staining); green – GFAP-positive astrocytes; red – Dox-PLGA-Cy5.5. Scale bars: 500 μm (A), 100 μm (B), 50 μm (C). (For interpretation of the references to color in this figure legend, the reader is referred to the web version of this article.)

These data strongly suggest that under the conditions used in the present study (the dose and especially the route of administration) the presence of mannitol in the formulation is not associated with BBB disruption and therefore is not likely to contribute to the antitumor effect of doxorubicin, both free and nanoparticle-bound.

3.6. Evaluation of brain distribution of fluorescently labeled Dox-PLGA nanoparticles

Although doxorubicin exhibits inherent fluorescent properties, its fluorescence intensity is quite variable depending on a number of factors such as local microenvironment, interaction with cellular components, and concentration (Mohan and Rapoport, 2010). In particular, doxorubicin molecules tend to self-associate at high concentrations resulting in fluorescence self-quenching. Quenching of doxorubicin fluorescence also occurs upon DNA binding. These phenomena complicate interpretation of doxorubicin fluorescence measurements.

Therefore, for better visualization in tumor-bearing rats using scanning laser confocal microscopy (SLCM), the doxorubicin-loaded nanoparticles were additionally labeled with Cy5.5, a far-red emitting fluorescent dye with the fluorescence properties that allow distinguishing it from doxorubicin (emission wavelengths of 661 nm and 597 nm, respectively). To prevent the leakage of the dye during the experiments Cy5.5 was covalently bound to the carboxylic end group (PLGA-Cy5.5). Stable attachment of Cy5.5 to the polymer was confirmed previously by the GPC analysis (Malinovskaya et al., 2017). Accordingly, no release of the dye from the nanoparticles has been observed during 72 h of incubation in PBS at 37 °C (data not shown). The physicochemical parameters of the Dox-PLGA-Cy5.5 nanoparticles (mean diameter 114 nm, PDI 0.196 ± 0.008; zeta potential −14.9 mV) were similar to those of the Dox-PLGA-p.s. sample used for evaluation of the anti-tumor effect. Although the Cy5.5 fluorescence intensity is considerably higher than that of doxorubicin, this double staining of the Dox-PLGA-Cy5.5 nanoparticles has previously enabled the visualization

of the path of both, the nanoparticles and the drug in an intracellular environment (Malinovskaya et al., 2017).

The intratumoral distribution of the doxorubicin-loaded PLGA nanoparticles coated with poloxamer 188 was investigated by confocal microscopy on day 14 post tumor implantation. As seen in Fig. 6, the tumor exhibited a highly heterogeneous microstructure. The Dox-PLGA-Cy5.5 nanoparticles coated with P188 effectively accumulated in the tumor 2 h post administration. The distribution patterns of doxorubicin and PLGA-Cy5.5 nanoparticles (as shown by Cy5.5 fluorescence) were slightly different (Fig. 6D and E), which could be due to partial release of doxorubicin from the nanoparticles at the time of analysis. At the same time, colocalization of doxorubicin with Cy5.5-labeled nanoparticles (Fig. 6A) demonstrated that after 2 h certain amounts of doxorubicin still were bound to the nanoparticles, which correlated with the doxorubicin release data (Fig. 2). Similar phenomenon was observed previously in the study of the Dox-PLGA-Cy5.5 internalization in the U87 cells: after 1 h the PLGA-Cy5.5 nanoparticles were still localized in the *endo*-lysosomal compartment, whereas a certain amount of doxorubicin at the same time was visible in the cell nuclei (Malinovskaya et al., 2017).

As expected, the accumulation of the nanoparticles was visibly higher in the tumor regions than in the normal brain tissues. This phenomenon obviously can be explained by the aforementioned increase of the BBB permeability due to tumor growth. However, staining of the brain sections of intact (control) animals with the antibodies to beta III-tubulin (neuronal marker) and GFAP (astrocyte marker) also revealed the colocalization of PLGA-Cy5.5 and doxorubicin fluorescence in neurons of hippocampus (Fig. 7), which indicated the ability of the nanoparticles to penetrate into the brain areas protected by the BBB. The nanoparticles were also found in the neurons of neocortex and cerebellum (Purkinje cells, Fig. 8).

This observation correlates with the results of previous studies, where similar PLGA nanoparticles labeled with DiI and coated with poloxamer 188 were visible in the neurons also 2 h post administration (Zybina et al., 2018). Other authors also observed the internalization of the vectorized nanoparticles in different subpopulations of neurons already 30 min post intravenous administration, whereas colocalization of the nanoparticles with astrocytes was observed only very rarely (Zensi et al., 2009; Tosi et al., 2014)). The astrocytes may have low phagocytic activity but they are known to form multiple intercellular connections. It is possible that the quick appearance of the nanoparticles in the neurons is explained by the ability of astrocytes to quickly carry the nanoparticles through the brain via efficient cytoplasmic routes (Begley, 2012). Importantly, in the chronic toxicity study of Dox-PLGA no signs of neurological toxicity were observed (Pereverzeva et al., 2018).

Overall, the results of the microscopical investigation correlate well with the higher anti-tumor effect of the nanoparticle-bound doxorubicin as compared to free drug that could be explained the ability of the nanoparticles to deliver the drug across the BBB and into the peritumoral areas.

In conclusion, the optimization of the preparation procedure that involved the replacement of PVA 30–70 kDa with the presumably safer low molecular mass PVA 9–10 kDa and the modification of the external emulsion medium and homogenization conditions during final emulsification step enabled the preparation of doxorubicin-loaded PLGA nanoparticles with a high encapsulation efficiency and a size of ~110 nm that is suitable for sterilization by membrane filtration. This technology was successfully scaled up with the batch volume increase from 60 ml to 1500 ml. The scaled-up process yielded an excellent reproducibility with very low inter-batch variations. The anti-tumor efficacy of the optimized formulation and the ability of the nanoparticles to penetrate into the intracranial tumor and in the normal brain tissue were unequivocally confirmed by the in vivo experiments. Furthermore, in the preclinical study, the optimized formulation exhibited a favorable toxicological profile characterized by reduced hematological, cardiac,

and testicular toxicity as compared to the conventional doxorubicin formulation (Pereverzeva et al., 2018).

These important steps of pharmaceutical development of the Dox-PLGA formulation enabled its translation into clinical trials as the nanomedicine for the chemotherapy of glioblastoma (Filon et al., 2017).

Declaration of Competing Interest

The authors declare that they have no known competing financial interests or personal relationships that could have appeared to influence the work reported in this paper.

Acknowledgment

References

Alyane, M., Barratt, G., Lahouela, M., 2016. Remote loading of doxorubicin into liposomes by transmembrane pH gradient to reduce toxicity toward H9c2 cells. Saudi Pharm. J. 24 (2), 165–175.

Ambruosi, A., Khalansky, A.S., Yamamoto, H., Gelperina, S.E., Begley, D.J., et al., 2006. Biodistribution of polysorbate 80-coated doxorubicin-loaded [14C]-poly(butyl cyanoacrylate) nanoparticles after intravenous administration to glioblastoma-bearing rats. J. Drug Target. 14, 97–105.

Athanasiou, K.A., Niederauer, G.G., Agrawal, C.M., 1996. Sterilization, toxicity, biocompatibility and clinical applications of polylactic acid polyglycolic acid copolymers. Biomaterials 17 (2), 93e102.

Bak, A., Podgórska, W., 2013. Drop breakage and coalescence in the toluene/water dispersions with dissolved surface active polymers PVA 88% and PVA 98%. Chem. Eng. Res. Des. 91, 2142–2155.

Bak, A., Podgórska, W., 2016. Influence of poly(vinyl alcohol) molecular weight on drop coalescence and breakage rate. Chem. Eng. Res. Des. 108, 88–100.

Begley, D.J., 2012. Brain superhighways. Sci. Transl. Med. 4 (147), 147fs29. https://doi.org/10.1126/scitranslmed.3004611.

Beijnen, J.H., van der Houwen, O.A.G.J., Underberg, W.J.M., 1986. Aspects of the degradation kinetics of doxorubicin in aqueous solution. Int. J. Pharm. 32, 123–131.

Birnbaum, D., Kosmala, J., Brannon-Peppas, L., 2000. Optimization of preparation techniques for poly(lactic acid-co-glycolic acid). J. Nanoparticle Res. 2, 173–181.

Bittner, B., Mäder, K., Kroll, C., Borchert, H.H., Kissel, T., 1999. Tetracycline-HCl-loaded poly(DL-lactide-co-glycolide) microspheres prepared by a spray drying technique: influence of gamma-irradiation on radical formation and polymer degradation. J. Control. Release 59, 23–32.

Cagel, M., Grotz, E., Bernabeu, E., Moretton, M.A., Chiappetta, D.A., 2017. Doxorubicin: nanotechnological overviews from bench to bedside. Drug Discov. Today 22 (2), 270–281. https://doi.org/10.1016/j.drudis.2016.11.005.

Caliş, S., Bozdag, S., Kaş, H.S., Tunçay, M., Hincal, A.A., 2002. Influence of irradiation sterilization on poly(lactide-co-glycolide) microspheres containing anti-inflammatory drugs. Farmaco 57 (1), 55–62.

Chen, K.B., Wei, V.C., Yen, L.F., Poon, K.S., Liu, Y.C., Cheng, K.S., Chang, C.S., Lai, T.W., 2013. Intravenous mannitol does not increase blood-brain barrier permeability to inert dyes in the adult rat forebrain. NeuroReport 24 (6), 303–307. https://doi.org/10.1097/WNR.0b013e32835f8acb.

Cho, E.J., Holback, H., Liu, K.C., Abouelmagd, S.A., Park, J., Yeo, Y., 2013. Nanoparticle characterization: state of the art, challenges, and emerging technologies. Mol. Pharm. 10, 2093–2110.

Cielecka-Piontek, J., Jelińska, A., Zajac, M., Sobczak, M., Bartold, A., Oszczapowicz, I., 2009. A comparison of the stability of doxorubicin and daunorubicin in solid state. J. Pharm. Biomed. Anal. 50 (4), 576–579.

Dorati, R., Colonna, C., Serra, M., Genta, I., Modena, T., Pavanetto, F., Perugini, P., Conti, B., 2008. γ-Irradiation of PEGd, lPLA and PEG-PLGA multiblock copolymers: I. Effect of irradiation doses. AAPS PharmSciTech. 9 (2), 718.

Eidel, O., Burth, S., Neumann, J.-O., Kieslich, P.J., Sahm, F., Jungk, C., et al., 2017. Tumor infiltration in enhancing and non-enhancing parts of glioblastoma: a correlation with histopathology. PLoS ONE 12 (1), e0169292. https://doi.org/10.1371/journal.pone.0169292.

Esquenazi, Y., Lo, V.P., Lee, K., 2017. Critical care management of cerebral edema in brain tumors. J. Intensive Care Med. 32 (1), 15–24. https://doi.org/10.1177/0885066615619618.

Fernández-Carballido, A., Herrero-Vanrell, R., Molina-Martínez, I.T., Pastoriza, P., 2004. Sterilized ibuprofen-loaded poly(D, L-lactide-co-glycolide) microspheres for intra-articular administration: effect of gamma-irradiation and storage. J. Microencapsul. 21, 653–665.

Filon, Olga, Krivorotko, Petr, Kobyakov, Grigory, Razjivina, Viktoria, Maximenko, Olga, Gelperina, Svetlana, Kreuter, Joerg, 2017. A phase I study of safety and pharmacokinetics of NanoBB-1-Dox in patients with advanced solid tumors. J. Clin. Oncol. 35

(15_suppl). https://doi.org/10.1200/JCO.2017.35.15_suppl.e13537.

Fornaguera, C., Solans, C., 2017. Methods for the in vitro characterization of nanomedicines – biological component interaction. J. Pers. Med. 7, 2. https://doi.org/10.3390/jpm7010002.

Gelperina, S., Maksimenko, O., Khalansky, A., Vanchugova, L., Shipulo, E., Abbasova, K., Berdiev, R., Wohlfart, S., Chepurnova, N., Kreuter, J., 2010. Drug delivery to the brain using surfactant-coated poly(lactide-co-glycolide) nanoparticles: influence of the formulation parameters. Eur. J. Pharm. Biopharm. 74 (2), 157–163.

Gerstner, E.R., Chen, P.-J., Wen, P.Y., Jain, R.K., Batchelor, T.T., Sorensen, G., 2010. Infiltrative patterns of glioblastoma spread detected via diffusion MRI after treatment with cediranib. Neuro-Oncol. 12 (5), 466–472. https://doi.org/10.1093/neuonc/nop051.

Hekmatara, T., Bernreuther, C., Khalansky, A.S., Theisen, A., Weissenberger, J., Matschke, J., Gelperina, S., Kreuter, J., Glatzel, M., 2009. Efficient systemic therapy of rat glioblastoma by nanoparticle-bound doxorubicin is due to antiangiogenic effects. Clin. Neuropathol. 28, 153–164.

von Holst, H., Knochenhauer, E., Blomgren, H., Collins, V.P., Ehn, L., Lindquist, M., Norén, G., Peterson, C., 1990. Uptake of adriamycin in tumour and surrounding brain tissue in patients with malignant gliomas. Acta Neurochir. (Wien) 104 (1–2), 13–16.

Janssen, M.J.H., Crommelin, D.J.A., Storm, G., Hulshoff, A., 1985. Doxorubicin decomposition on storage. Effect of pH, type of buffer and liposome encapsulation. Int. J. Pharm. 23, 1–11.

Kaczmarek, A., Cielecka-Piontek, J., Garbacki, P., Lewandowska, K., Bednarski, W., Barszcz, B., Zalewski, P., Kycler, W., Oszczapowicz, I., Jelińska, A., 2013. Radiation sterilization of anthracycline antibiotics in solid state. Sci. World J. 2013, 258758. https://doi.org/10.1155/2013/258758.eCollection.

Kaneo, Y., Hashihama, S., Kakinoki, A., Tanaka, T., Nakano, T., Ikeda, Y., 2005. Pharmacokinetics and biodisposition of poly(vinyl alcohol) in rats and mice. Drug Metab. Pharmacokinet. 20 (6), 435–442.

Kanwal, U., Irfan Bukhari, N., Ovais, M., Abass, N., Hussain, K., Raza, A., 2018. Advances in nano-delivery systems for doxorubicin: an updated insight. J. Drug Target. 26 (4), 296–310. https://doi.org/10.1080/1061186X.2017.1380655.

Kataoka, K., Matsumoto, T., Yokoyama, M., Okano, T., Sakurai, Y., Fukushima, S., Okamoto, K., Kwon, G.S., 2000. Doxorubicin-loaded poly(ethylene glycol)-poly(β-benzyl-L-aspartate) copolymer micelles: their pharmaceutical characteristics and biological significance. J. Control. Release 64 (1–3), 143–153.

Kaushik, D., Bansal, G., 2015. Four new degradation products of doxorubicin: an application of forced degradation study and hyphenated chromatographic techniques. J. Pharm. Anal. 5 (5), 285–295.

Kreuter, J., 2014. Drug delivery to the central nervous system by polymeric nanoparticles: what do we know? Adv. Drug Deliv. Rev. 71, 2–14. https://doi.org/10.1016/j.addr.2013.08.008.

Lee, L., Norton, I.T., 2013. Comparing droplet breakup for a high-pressure valve homogeniser and a Microfluidizer for the potential production of food-grade nanoemulsions. J. Food Eng. 114, 158–163.

Lemée, J.-M., Clavreul, A., Menei, P., 2015. Intratumoral heterogeneity in glioblastoma: don't forget the peritumoral brain zone. Neuro-Oncol. 17 (10), 1322–1332. https://doi.org/10.1093/neuonc/nov119.

van Linde, M.E., Brahm, C.G., de Witt Hamer, P.C., Reijneveld, J.C., Bruynzeel, A.M.E., Vandertop, W.P., van de Ven, P.M., Wagemakers, M., van der Weide, H.L., Enting, R.H., Walenkamp, A.M.E., Verheul, H.M.W., 2017. Treatment outcome of patients with recurrent glioblastoma multiforme: a retrospective multicenter analysis. J. Neurooncol. 135 (1), 183–192. https://doi.org/10.1007/s11060-017-2564-z.

Liu, M., Zheng, Yu., Li, J., Chen, S., Liu, Y., Li, J., Li, B., Zhang, Zh., 2017. Effects of molecular weight of PVA on formation, stability and deformation of compound droplets for ICF polymer shells. Nucl. Fusion 57 016018 (10, pp).

Loo, S.C.J., Ooi, C.P., Boey, Y.C.F., 2004. Radiation effects on poly(lactide-co-glycolide) (PLGA) and poly(L-lactide) (PLLA). Polym. Degrad. Stab. 83 (2), 259–265.

Maksimenko, O., Pavlov, E., Toushov, E., Molin, A., Stukalov, Y., Prudskova, T., Feldman, V., Kreuter, J., Gelperina, S., 2008. Radiation sterilisation of doxorubicin bound to poly(butyl cyanoacrylate) nanoparticles. Int. J. Pharm. 356, 325–332.

Malinovskaya, Y., Melnikov, P., Baklaushev, V., Gabashvili, A., Osipova, N., Mantrov, S., Ermolenko, Y., Maksimenko, O., Gorshkova, M., Balabanyan, V., Kreuter, J., Gelperina, S., 2017. Delivery of doxorubicin-loaded PLGA nanoparticles into U87 human glioblastoma cells. Int. J. Pharm. 524 (1–2), 77–90.

Mao, L., Yang Ji, Xu.D., Yuan, F., Gao, Y., 2010. Effects of homogenization models and emulsifiers on the physicochemical properties of β-carotene nanoemulsions. J. Dispersion Sci. Tech. 31 (7), 986–993. https://doi.org/10.1080/01932690903224482.

Marczak, A., Kowalczyk, A., Wrzesień-Kus, A., Robak, T., Jóźwiak, Z., 2006. Interaction of doxorubicin and idarubicin with red blood cells from acute myeloid leukaemia patients. Cell Biol. Int. 30 (2), 127–132.

Mohan, P., Rapoport, N., 2010. Doxorubicin as a molecular nanotheranostic agent: effect of doxorubicin encapsulation in micelles or nanoemulsions on the ultrasound-mediated intracellular delivery and nuclear trafficking. Mol. Pharm. 7 (6), 1959–1973.

Montanari, L., Cilurzo, F., Valvo, L., Faucitano, A., Buttafava, A., Groppo, A., Genta, I., Conti, B., 2001. Gamma irradiation effects on stability of poly(lactide-co-glycolide) microspheres containing clonazepam. J. Control. Release 75, 317–330.

Murakami, H., Kawashima, Y., Niwa, T., Hino, T., Takeuchi, H., Kobayashi, M., 1997. Influence of the degrees of hydrolyzation and polymerization of poly(vinylalcohol) on the preparation and properties of poly(DL-lactide-co-glycolide) nanoparticles. Int. J. Pharm. 149, 43–49.

Neun, B.W., Dobrovolskaia, M.A., 2011. Method for in vitro analysis of nanoparticle

thrombogenic properties. Methods Mol. Biol. 697, 225–235. https://doi.org/10.1007/978-1-60327-198-1_24.

Ostrom, Q.T., Gittleman, H., Truitt, G., Boscia, A., Kruchko, C., Barnholtz-Sloan, J.S., 2018. CBTRUS statistical report: primary brain and other central nervous system tumors diagnosed in the United States in 2011–2015. Neurooncol. 20, v1–v86. https://doi.org/10.1093/neuonc/noy131.

Pereverzeva, E., Treschalin, I., Treschalin, M., Arantseva, D., Ermolenko, Y., Kumskova, N., Maksimenko, O., Balabanyan, V., Kreuter, J., Gelperina, S., 2018. Toxicological study of doxorubicin-loaded PLGA nanoparticles for the treatment of glioblastoma. Int. J. Pharm. 554, 161–178. https://doi.org/10.1016/j.ijpharm.2018.11.014.

Petrecca, K., Guiot, M.C., Panet-Raymond, V., Souhami, L., 2013. Failure pattern following complete resection plus radiotherapy and temozolomide is at the resection margin in patients with glioblastoma. J. Neurooncol. 111 (1), 19–23. https://doi.org/10.1007/s11060-012-0983-4.

Riina, H.A., Fraser, J.F., Fralin, S., Knopman, J., Scheff, R.J., Boockvar, J.A., 2009. Superselective intraarterial cerebral infusion of bevacizumab: a revival of interventional neuro-oncology for malignant glioma. J. Exp. Ther. Oncol. 8 (2), 145–150.

Sahoo, S.K., Panyam, J., Prabha, S., Labhasetwar, V., 2002. Residual polyvinyl alcohol associated with poly (D, L-lactide-co-glycolide) nanoparticles affects their physical properties and cellular uptake. J. Control. Release 82 (1), 105–114.

Sanson, C., Schatz, C., Le Meins, J.F., Soum, A., Thévenot, J., Garanger, E., Lecommandoux, S., 2010. A simple method to achieve high doxorubicin loading in biodegradable polymersomes. J. Control. Release 147 (3), 428–435. https://doi.org/10.1016/j.jconrel.2010.07.123.

Shergalis, A., Bankhead 3rd, A., Luesakul, U., Muangsin, N., Neamati, N., 2018. Current challenges and opportunities in treating glioblastoma. Pharmacol. Rev. 70 (3), 412–445. https://doi.org/10.1124/pr.117.014944.

Sintzel, M.B., Merkli, A., Tabatabay, C., Gurny, R., 1997. Influence of irradiation sterilization on polymers used as drug carriers: a review. Drug Dev. Ind. Pharm. 23 (9), 857e78.

Steiniger, S.C., Kreuter, J., Khalansky, A.S., Skidan, I.N., Bobruskin, A.I., Smirnova, Z.S., Severin, S.E., Uhl, R., Kock, M., Geiger, K.D., Gelperina, S.E., 2004. Chemotherapy of glioblastoma in rats using doxorubicin-loaded nanoparticles. Int. J. Cancer 109, 759–767.

Tabata, Y., Murakami, Y., Ikada, Y., 1998. Tumor accumulation of poly(vinyl alcohol) of different sizes after intravenous injection. J. Control. Release 50 (1–3), 123–133.

van Tellingen, O., Yetkin-Arik, B., de Gooijer, M.C., Wesseling, P., Wurdinger, T., de Vries, H.E., 2015. Overcoming the blood-brain tumor barrier for effective glioblastoma treatment. Drug Resist Updat. 19, 1–12. https://doi.org/10.1016/j.drup.2015.02.002.

Tomita, T., 1991. Interstitial chemotherapy for brain tumors: review. J. Neurooncol. 10, 57–74.

USP 29 Monograph. Polyvinyl alcohol. http://ftp.uspbpep.com/v29240/usp29nf24s0_m66990.html.

Tosi, G., Vilella, A., Chhabra, R., Schmeisser, M.J., Boeckers, T.M., Ruozi, B., Vandelli, M.A., Forni, F., Zoli, M., Grabrucker, A.M., 2014. Insight on the fate of CNS-targeted nanoparticles. Part II: intercellular neuronal cell-to-cell transport. J. Control. Release 117, 96–107.

Vandervoort, J., Ludwig, A., 2002. Biocompatible stabilizers in the preparation of PLGA nanoparticles: a factorial design study. Int. J. Pharm. 238, 77–92.

Varshney, L., Dodke, P.B., 2004. Radiation effect studies on anticancer drugs, cyclophosphamide and doxorubicin for radiation sterilization. Radiation Phys. Chem. 71, 1103–1111.

Vehlow, A., Cordes, N., 2013. Invasion as target for therapy of glioblastoma multiforme. BBA 1836 (2), 236–244. https://doi.org/10.1016/j.bbcan.2013.07.001.

Vigevani, A., Williamson, M.J., 1981. Doxorubicin. Anal. Prof. Drug Subst. 9, 245–274.

Volland, C., Wolff, M., Kissel, T., 1994. The influence of terminal gamma-sterilization on captopril containing poly(d, l-lactide-co-glycolide) microspheres. J. Control. Release 31, 293–305.

Voulgaris, S., Partheni, M., Karamouzis, M., Dimopoulos, P., Papadakis, N., Kalofonos, H.P., 2002. Intratumoral doxorubicin in patients with malignant brain gliomas. Am. J. Clin. Oncol. 25 (1), 60–64.

Williams, H.E., Huxley, J., Claybourn, M., Booth, J., Hobbs, M., Meehan, E., Clark, B., 2006. The effect of g-irradiation and polymer composition on the stability of PLG polymer and microspheres. Polym. Degrad. Stab. 91, 2171–2181.

Wohlfart, S., Bernreuther, C., Khalansky, A.S., Theisen, A., Weissenberger, J., Gelperina, S., Glatzel, M., Kreuter, J., 2009. Increased numbers of injections of doxorubicin bound to nanoparticles lead to enhanced efficacy against rat glioblastoma 101/8. J. Nanoneurosci. 1, 144–151.

Wohlfart, S., Khalansky, A.S., Gelperina, S., Maksimenko, O., Bernreuther, C., Glatzel, M., Kreuter, J., 2011. Efficient chemotherapy of rat glioblastoma using doxorubicin-loaded PLGA nanoparticles with different stabilizers. PLoS ONE 6 (5), e19121. https://doi.org/10.1371/journal.pone.0019121.

Yamaoka, T., Tabata, Y., Ikada, Y., 1995. Comparison of body distribution of poly(vinyl alcohol) with other water-soluble polymers after intravenous administration. J. Pharm. Pharmacol. 47 (6), 479–486.

Zensi, A., Begley, D., Pontikis, C., Legros, C., Mihoreanu, L., Wagner, S., Büchel, C., von Briesen, H., Kreuter, J., 2009. Albumin nanoparticles targeted with Apo E enter the CNS by transcytosis and are delivered to neurons. J. Control. Release 137, 78–86.

Zybina, A., Anshakova, A., Malinovskaya, J., Melnikov, P., Baklaushev, V., Chekhonin, V., Maksimenko, O., Titov, S., Balabanyan, V., Kreuter, J., Gelperina, S., Abbasova, K., 2018. Nanoparticle-based delivery of carbamazepine: a promising approach for the treatment of refractory epilepsy. Int. J. Pharm. 547 (1–2), 10–23.